The Canadian Mineralogist
Vol. 33, pp. 373-388 (1995)

ION-MICROPROBE ANALYSIS OF PYRITE, CHALCOPYRITE AND PYRRHOTITE FROM THE MOBRUN VMS DEPOSIT IN NORTHWESTERN QUEBEC: EVIDENCE FOR METAMORPHIC REMOBILIZATION OF GOLD

ADRIENNE C.L. LAROCQUE* AND C. JAY HODGSON
Department of Geological Sciences, Queen's University, Kingston, Ontario K7L 3N6

LOUIS J. CABRI AND JENNIFER A. JACKMAN
CANMET, 555 Booth Street, Ottawa, Ontario K1A 0G1

ABSTRACT

The Mobrun Zn–Cu–Ag–Au deposit, located in the Noranda District, in the Quebec segment of the Abitibi Greenstone Belt, is hosted mainly by felsic volcanic rocks of the Archean Blake River Group. Primary facies of mineralization in the Mobrun orebodies resulted from deposition and reworking of sulfides by synvolcanic hydrothermal fluids. Secondary facies of mineralization resulted from greenschist-grade metamorphism and related deformation, and locally overprinted the primary facies. The "invisible" (refractory) gold contents of pyrite, chalcopyrite and pyrrhotite in various facies were determined using a Cameca IMS–4f ion microprobe. Samples were sputtered with a Cs^+ primary beam, and negative secondary ions were measured. External standards of sulfides were implanted with ^{197}Au. Mass interferences were eliminated by operating in high-mass-resolution mode (M/ΔM in the range 2400 to 3900), giving rise to minimum limits of detections of 50 ppbw. Primary pyrite contains up to 10 ppmw gold, present as submicrometric inclusions of metallic gold, as well as very fine colloid-size or structurally bound gold. Concentrations of gold in associated secondary (recrystallized) pyrite range from 1 to 67% of the concentrations in primary pyrite. The results indicate that syngenetic gold is present in the Mobrun orebodies, and that metamorphic recrystallization resulted in its release from pyrite. The remobilized gold was deposited in tectonic veins as easily recoverable electrum and as "invisible" gold in secondary chalcopyrite. The partitioning of gold among various phases in secondary veins may have been influenced by the interaction between the remobilizing fluid and the assemblages of primary ore minerals.

Keywords: "invisible" gold, refractory gold, ion microprobe, SIMS, pyrite, chalcopyrite, pyrrhotite, electrum, remobilization, metamorphic recrystallization, volcanogenic massive sulfide, Mobrun, Noranda, Quebec.

SOMMAIRE

Le gisement à Zn–Cu–Ag–Au de Mobrun, situé dans le district de Noranda, dans le secteur québécois de la ceinture de roches vertes de l'Abitibi, est encaissé dans une suite de roches volcaniques, surtout felsiques, du Groupe de Blake River, d'âge archéen. Les faciès primaires de minéralisation dans les gîtes de sulfures massifs se sont formés par déposition et par modification des sulfures par des fluides hydrothermaux synvolcaniques. Les faciès secondaires de minéralisation se sont formés par métamorphisme dans le faciès schistes verts et par déformation contemporaine, et localement ont oblitéré les faciès primaires. Les teneurs en or "invisible" (réfractaire) de la pyrite, la chalcopyrite et la pyrrhotite dans plusieurs faciès de minéralisation ont été déterminées par microsonde ionique Cameca IMS–4f. Les échantillons ont été bombardés avec un faisceau d'ions primaires de Cs^+, et les ions négatifs secondaires émis ont été mesurés. Les étalons externes de sulfures ont été implantés avec l'isotope ^{197}Au. On a pu éliminer les interférences de masse par opération dans le mode de haute résolution de masses (M/ΔM de 2400 à 3900), ce qui a permis un seuil de détection minimum de 50 ppb (poids). La pyrite primaire contient jusqu'à 10 ppm d'or, soit incorporé dans la structure, soit en inclusions submicrométriques ou encore de taille colloïdale. La pyrite secondaire (recristallisée) contient entre 1 et 67% de la teneur en or de la pyrite primaire. Les résultats indiquent que l'or syngénétique est présent dans les gîtes de Mobrun, et que la recristallisation métamorphique a libéré l'or de la pyrite, et l'a deposé dans les veines d'origine tectonique sous forme d'électrum, facilement recouvrable, et d'or "invisible" dans la chalcopyrite secondaire. La répartition de l'or parmi les divers minéraux des veines secondaires dépendrait possiblement de l'interaction de la phase fluide et l'assemblage de minerais primaires.

Mots-clés: or "invisible", or réfractaire, microsonde ionique, spectrométrie de masse des ions secondaires, pyrite, chalcopyrite, pyrrhotite, électrum, remobilisation, recristallisation métamorphique, sulfures massifs volcanogéniques, Mobrun, Noranda, Québec.

---

* Present address: Department of Geological Sciences, The University of Manitoba, Winnipeg, Manitoba R3T 2N2.

INTRODUCTION

Two main types of Archean gold deposits occur in the Abitibi Greenstone Belt in northeastern Ontario and northwestern Quebec: (1) volcanogenic massive-sulfide (VMS) deposits, which formed synchronously with the host volcanic rocks and which contain gold; (2) structurally controlled vein and replacement deposits. The origin of gold in Archean VMS deposits is controversial, and three main views are held: (1) the gold was introduced syngenetically (*e.g.*, Huston & Large 1989), (2) the gold was introduced syngenetically, but its present distribution is the result of remobilization that occurred during metamorphism and tectonic deformation (*e.g.*, Tourigny *et al.* 1989, 1993, Healy & Petruk 1990), and (3) the gold was introduced epigenetically, as in most structurally controlled gold-only deposits (*e.g.*, Marquis *et al.* 1990).

Ion-microprobe analysis of sulfide minerals has been used for some time by process mineralogists for the characterization of sulfide ores (*e.g.*, Chryssoulis *et al.* 1985, 1986, 1987, Chryssoulis 1990, Chryssoulis & Cabri 1990, Cabri *et al.* 1991, Marion *et al.* 1991, Cabri 1992). However, the geological application of secondary-ion mass spectrometry (SIMS) to the analysis of sulfides for trace metals has been more recent (Arehart *et al.* 1991, 1993, Bakken *et al.* 1991, Hickmott & Baldridge 1991, Layne *et al.* 1991, Marion *et al.* 1992, Peng 1992, Larocque *et al.* 1992, 1993b, c, Neumayr *et al.* 1993). The purpose of this paper is to present the results of ion-microprobe analysis of sulfide minerals from the Mobrun VMS deposit in northwestern Quebec, and to discuss the implications of these results for the origin of gold in the deposit.

EVIDENCE FOR SYNGENETIC AND REMOBILIZED GOLD

The clearest evidence of syngenetic deposition of gold in massive-sulfide deposits comes from the identification of gold in actively forming and recently formed deposits on the seafloor. Hannington *et al.* (1986) documented anomalously high contents of gold (up to 1500 ppb) in samples from polymetallic sulfide deposits in the eastern Pacific Ocean. Samples containing up to 10 ppm gold have been recovered from the Manus Basin of Papua New Guinea (Scott & Binns 1992). Sulfide samples from the East Pacific Rise, Galapagos Rift, and southern Juan de Fuca Ridge contain up to 200 ppb gold (Bischoff *et al.* 1983). Auriferous sulfides have been collected on the Mid-Atlantic Ridge and the East Pacific Rise (Hannington & Scott 1988, 1989, and references therein). In addition, up to 200 ppb gold has been measured in sulfides from hydrothermal plumes issuing from seafloor vents along the East Pacific Rise (Hannington *et al.* 1991, and references therein).

There is also evidence for syngenetic deposition of gold in ancient VMS deposits. Kerr & Mason (1990) proposed that the deposit at the Horne mine in the Noranda camp was formed by synvolcanic hydrothermal processes operating during a period of Archean felsic volcanism. Although deformation resulted in small-scale remobilization of sulfides and gold into late quartz-bearing veinlets, they interpreted auriferous sulfides to have been deposited through subseafloor replacement of rhyolite tuffs. Huston & Large (1989) summarized the mineralogy and distribution of gold in selected VMS deposits in Canada, Australia, Japan, Sweden and Cyprus, in which gold is considered to occur mainly as inclusions or in "solid solution" in sulfide minerals (Huston & Large 1989), indicating that it was deposited synchronously with the primary sulfides.

The general view of remobilization brought about by metamorphism is that it is a process of dispersion rather than one of concentration. However, some studies suggest that the interaction of pre-existing mineralization with metamorphic fluids may have resulted in mobilization and concentration of elements into economic bodies. The case for late gold being derived by metamorphic remobilization of early gold has been argued by Tourigny *et al.* (1989, 1993) for the Bousquet No. 2 deposit in the Abitibi belt, where early mineralization and hydrothermal alteration resulted in auriferous massive-sulfide mineralization and associated argillic alteration. They suggested that remobilization of early sulfides during subsequent regional greenschist-facies metamorphism formed structurally controlled vein-type gold deposits. At the Trout Lake massive-sulfide deposit near Flin Flon, Manitoba, Healy & Petruk (1990) identified two textural types of gold alloy, as well as minor amounts of "invisible" gold (as determined by SIMS analyses) in pyrite and arsenopyrite. According to Healy & Petruk (1990), gold was released from pyrite following metablastesis, crystallizing as fracture-fillings in pyrite from locally migrating late metamorphic pore-fluids. In addition, anastomosing masses along the folded contacts between laminae of massive chalcopyrite and chlorite schist formed from metamorphic remobilization of coarse-grained free gold in the chalcopyrite-rich footwall ore. Huston *et al.* (1993) have documented the effects of metamorphic recrystallization on the composition of pyrite in a number of VMS deposits in Australia. Using proton-microprobe data, they concluded that recrystallization resulted in the release of gold and other trace elements from pyrite. Although they did not identify a potential sink for the remobilized gold, they documented important evidence for the release of gold during metamorphic recrystallization.

GEOLOGICAL SETTING OF THE MOBRUN MINE

The Mobrun deposit is one of a group of VMS deposits in the Noranda mining camp hosted by

interbedded mafic-to-felsic submarine volcanic rocks of the Archean Blake River Group (BRG; de Rosen-Spence 1976). The lower part of the BRG in the Noranda camp is a shield volcano, and the upper part is a caldera complex (Gibson & Watkinson 1990). Most of the massive-sulfide deposits of the camp occur along synvolcanic faults within and along the caldera margin. The Mobrun deposit occurs in the upper part of the stratigraphic succession (Cycle V of Spence & de Rosen-Spence 1975) about 7 km northwest of the caldera margin.

The structural history of the area includes two main periods of deformation (Dimroth *et al.* 1983a, Hubert *et al.* 1984). The Noranda camp is located on the gently dipping upright limb of one of a number of large-scale northwest-trending folds (*D*1). Associated *D*1 faults typically consist of bedding-parallel zones of schistosity. The main cleavage-forming event was *D*2, which resulted in east-trending folds and an associated domainal cleavage. Metamorphic grades range from prehnite–pumpellyite to greenschist facies (Jolly 1980, Dimroth *et al.* 1983b, Gélinas *et al.* 1984). Amphibolite-facies assemblages that overprint greenschist assemblages occur in contact-metamorphic aureoles of syn- to late-tectonic intrusions (Gélinas *et al.* 1984). In the Noranda area, greenschist-facies assemblages dominate.

The Mobrun mine is located 30 km northeast of Rouyn–Noranda (Fig. 1). The deposit is hosted by felsic, intermediate and mafic lava flows, and felsic and intermediate pyroclastic rocks, that strike 110° to 120° and dip subvertically to the south (Caumartin & Caillé 1990, Barrett *et al.* 1992, Larocque & Hodgson 1993). It consists of three massive-sulfide complexes: the 1100 orebody, the Main lens, and the Satellite lens complex (Fig. 1). The respective grades and tonnages

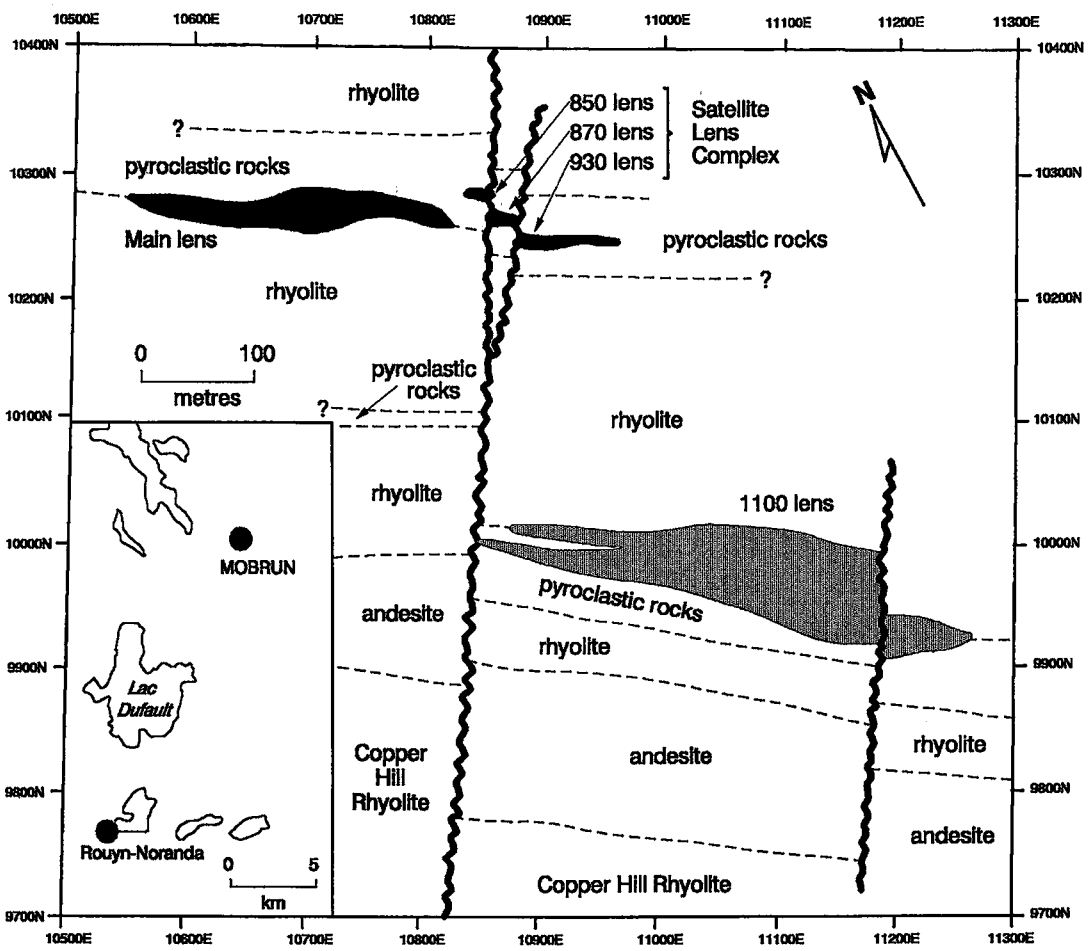

FIG. 1. Geology of the Mobrun deposit, modified from Caumartin & Caillé (1990). Orebodies in black are near-surface; orebody at depth is stippled. Inset: location map.

of the orebodies are listed in Table 1. The 1100 orebody is stratigraphically lowest, and consists of four separate massive-sulfide lenses, designated A, B, C and D (see Larocque *et al.* 1993a, Fig. 4). The B lens contains the bulk of the mineralization in the 1100 orebody; it has a lateral extent of 300 m, and extends downward from 360 m below surface to an unknown depth. The Main lens has a lateral extent of 350 m and a present vertical extent of approximately 200 m (the upper part of the orebody has been removed by erosion). The Satellite lens complex comprises three small massive-sulfide bodies representing three parts of one originally continuous lens offset by northeast-striking faults (Fig. 1).

Alteration affecting the rocks that host the orebodies consists of sericitization, silicification, and chloritization (Caumartin & Caillé 1990, Riopel *et al.* 1990, Barrett *et al.* 1992). In addition, synvolcanic hydrothermal carbonate alteration has been recognized in the rocks hosting the 1100 orebody (Larocque & Hodgson 1993). A regional schistosity (*S*1) oriented parallel to stratigraphy is best developed in localized zones of altered rocks enveloping the lenses of massive sulfides, and is cut by a second schistosity (*S*2) striking east–west and dipping steeply to the south (Caumartin & Caillé 1990, Riopel *et al.* 1990).

Ore Petrography and Geochemistry

The main sulfide minerals in the Mobrun orebodies are pyrite, sphalerite, and chalcopyrite (Figs. 2, 3), with minor galena, arsenopyrite, digenite and tetrahedrite. Electrum, mainly in veins, also occurs as inclusions in pyrite and sphalerite (Larocque & Hodgson 1991, Larocque *et al.* 1993a). In the 1100 orebody, pyrrhotite is abundant in the stratigraphically lower part of the lens. Quartz, carbonate, chlorite and muscovite are the main gangue minerals.

Based on mineralogical, textural, and structural characteristics, thirteen different facies of mineralization have been identified at Mobrun (Larocque 1993, Larocque *et al.* 1993a). The end-member types of mineralization summarized in Table 2 may show gradational or overprinting relationships. These facies represent mappable subunits of the massive-sulfide bodies, and have genetic significance, as they resulted from specific depositional or deformational processes. Primary facies resulted from deposition and reworking of sulfides by synvolcanic hydrothermal fluids, and are similar to mineralization in modern seafloor and Kuroko deposits [see Larocque (1993) and Larocque *et al.* (1993a) for specific criteria for identification of facies]. Secondary facies formed as a result of metamorphism and deformation, and locally overprint the primary facies. Examples of some primary and secondary facies of mineralization are illustrated in Figures 2 and 3 (see also Larocque *et al.* 1995, Fig. 1).

Each of the orebodies exhibits zonation of the facies of mineralization. In addition to large-scale zonation of facies (Larocque *et al.* 1993a, Figs. 4 to 6), textural zonation has been observed on hand-specimen and thin-section scales (Figs. 2, 3). There is excellent preservation of the primary facies of mineralization in the Main and Satellite lenses, given the state of deformation of rocks hosting the Mobrun orebodies. Although the 1100 orebody also contains primary textures, the development of secondary facies is more pronounced, owing to its more severe deformation and metamorphic recrystallization (Larocque *et al.* 1993a). The distribution of *dominant* facies of mineralization is similar in each of the orebodies, although the distribution in the 1100 orebody is complicated by the fact that the B lens comprises two coalesced massive-sulfide lenses. In general, each lens or sublens comprises a basal zone of granular mineralization, a core zone of massive pyrite, and an upper zone of granular mineralization that grades upward into banded pyrite + sphalerite or massive sphalerite. Pyrrhotite-bearing facies are abundant in the footwall to the B and C lenses of the 1100 orebody (Larocque 1993). Overprinting secondary facies consist mainly of transgressive veins developed toward the flanks of the core of massive pyrite in the Main and Satellite lenses and the western part of the B lens of the 1100 orebody. The veins generally contain quartz and chalcopyrite, and may contain electrum. Recrystallized massive pyrite dominates in the eastern part of the B lens, and is present as patches in the flank areas of the Main and Satellite lenses (Larocque *et al.* 1993a).

Hand samples containing primary facies of mineralization contain up to 5 ppm gold in the Main lens and up to 10 ppm gold in the Satellite lens complex. In both the Main and Satellite lenses, primary facies contain 10 to 60 ppm silver. In the 1100 orebody, primary facies contain up to 10 ppm gold, and up to 160 ppm silver. In all orebodies, samples with secondary veins exhibit significantly higher concentrations of gold, silver, or both, owing to the presence of electrum. The maximum concentrations of gold and silver are lowest in the Satellite lens complex (23 and 137 ppm, respectively) and highest in the 1100 lens (245 and 780 ppm, respectively; Larocque *et al.* 1993a).

TABLE 1. ORE RESERVES, MOBRUN MINE[1]

OREBODY	TONNES	% Cu	% Zn	g/t Ag	g/t Au	Au/Ag
SATELLITE[2]	179,000	1.20	2.41	42.27	4.98	0.12
MAIN[2]	955,000	0.81	2.44	30.30	2.27	0.07
1100[3]	7,572,000	0.84	5.87	42.50	1.75	0.04
TOTAL	8,706,000	0.84	5.42	41.12	1.87	0.05

[1] Provided by Ressources Audrey Inc. [2] Proven reserves, February 1, 1989. [3] Probable reserves, October 25, 1991.

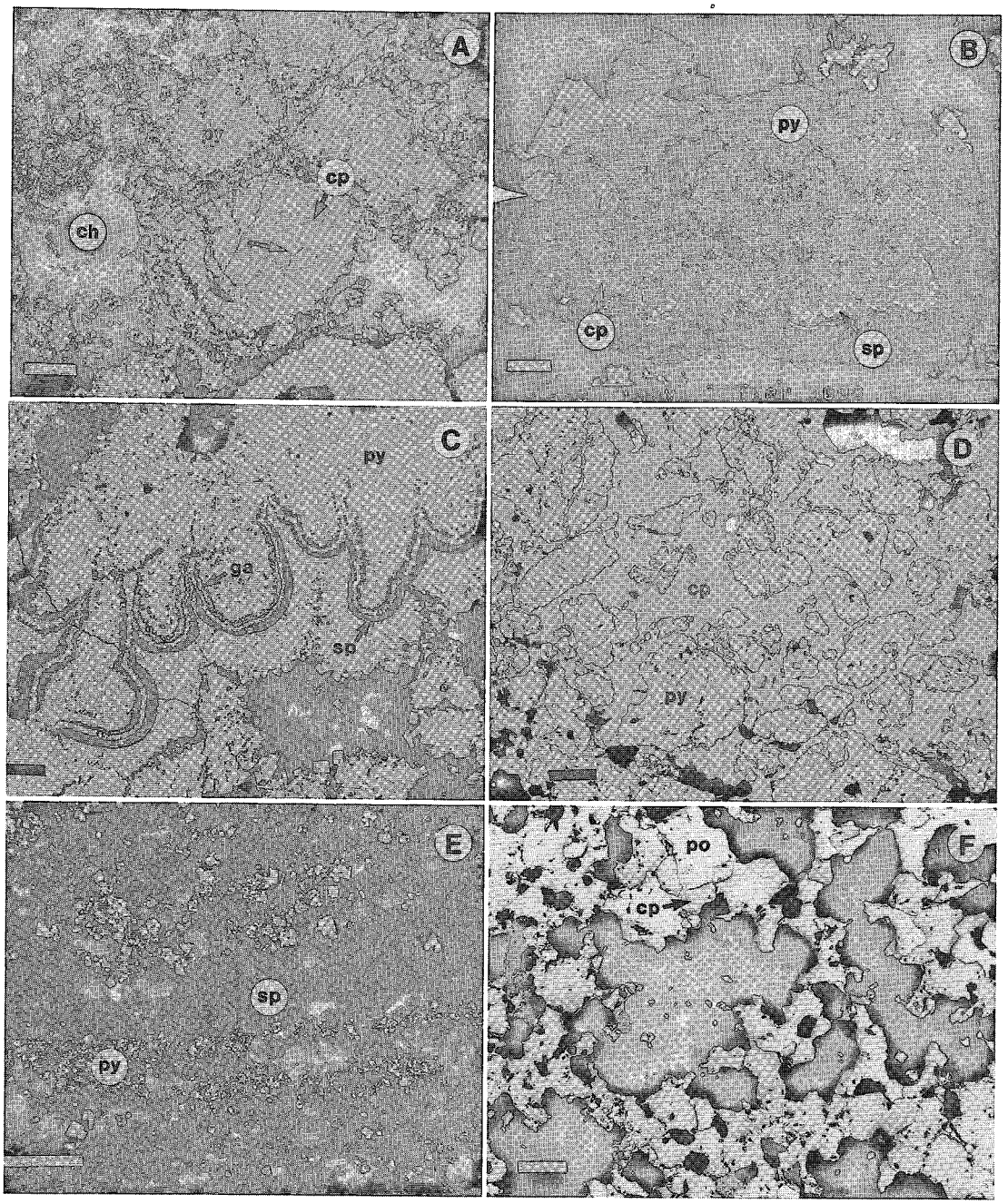

FIG. 2. Examples of primary facies of mineralization from the Mobrun deposit. All photos except for B are reflected-light photomicrographs. Abbreviations are as follows: pyrite (py), pyrrhotite (po), chalcopyrite (cp), sphalerite (sp), galena (ga), chlorite (ch). Scale bars in lower left corner; lengths of bars in parentheses. A) Granular pyrite with concentric colloform banding of chalcopyrite, in a matrix of chlorite. Arrow indicates location of secondary-ion image in Figure 11 (250 μm). B) Back-scatter scanning electron microscope photograph of spheroidal aggregate of pyrite with colloform banding defined by chalcopyrite and sphalerite (100 μm). C) Massive fine pyrite with colloform bands of sphalerite and galena (100 μm). D) Pyrite partly replaced by chalcopyrite in massive pyrite – chalcopyrite facies (200 μm). E) Massive sphalerite with thin bands of pyrite (500 μm). F) Stringer mineralization consisting of chalcopyrite and pyrrhotite with "swiss cheese" texture replacing altered wallrock (100 μm).

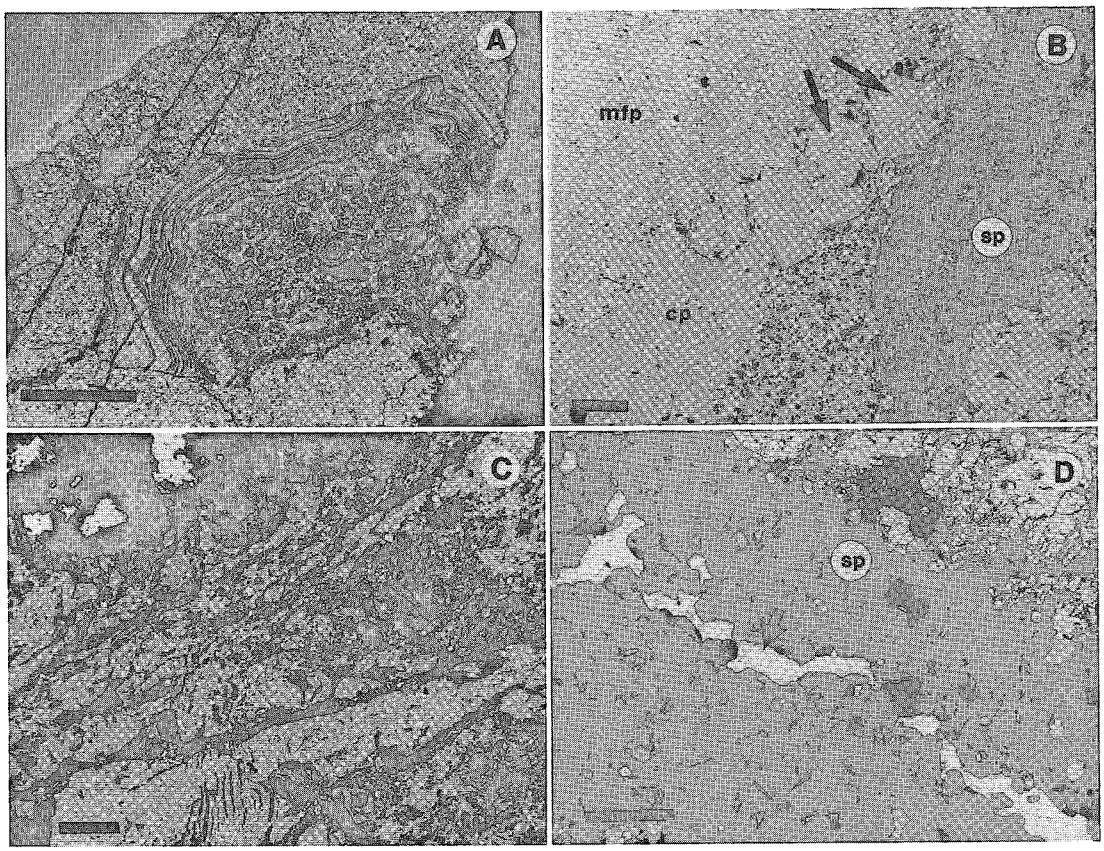

FIG. 3. Examples of secondary facies of mineralization from the Mobrun deposit. Abbreviations as in Figure 2. A) Primary colloform banding truncated by massive coarse (recrystallized) pyrite (500 μm). B) Primary massive fine pyrite (mfp) cut by secondary vein containing coarse euhedral pyrite (arrows), chalcopyrite, and sphalerite (250 μm). C) Foliated pyrite in matrix of carbonate, chlorite, and quartz (500 μm). D) Vein of electrum (arrow) in sphalerite (200 μm).

METHODOLOGY

Sampling and bulk chemical analyses

In situ sampling of ore was carried out in accessible underground areas of the Main and Satellite lenses in 1990 and 1991. In addition, drill core from the Satellite lens complex and 1100 orebody was logged and sampled (core from the Main lens had been used for metallurgical testing and was not available for sampling). Splits (50–300 g) of bulk samples were analyzed for Cu, Zn, and Ag (by atomic absorption spectroscopy) and Au (by fire assay) at the lab at Mobrun. Polished sections of ore were prepared for petrographic study and analysis by electron microprobe (EPMA), scanning electron microscope (SEM), and secondary-ion mass spectrometry (SIMS).

Ion-microprobe analysis

The calibration and operation of SIMS have been discussed by McIntyre *et al.* (1984), Chryssoulis *et al.* (1989), Cabri & Chryssoulis (1990), and Cabri *et al.* (1989, 1991), among others. For this study, a Cameca IMS–4f ion microprobe was used to quantify the gold content of sulfide minerals from the various lenses of ore at the Mobrun mine. Experimental parameters are summarized in Table 3. For their ion-microprobe study of gold content of pyrite, Chryssoulis *et al.* (1987) operated in high-mass-resolution mode with an energy offset to eliminate a mass interference with $^{197}CsS_2^-$ (Fig. 4) and achieved minimum detection-limits (MDL) of 500 ppb. For our study, operation in high-mass-resolution mode alone yielded good dynamic range (peak/background) and lower detection-limits

TABLE 2. FACIES OF MINERALIZATION*

PRIMARY FACIES	Formed by deposition and reworking of sulfides by synvolcanic hydrothermal fluids (syngenetic/diagenetic)
Bedded Pyritic Mineralization	- μm-scale pyrite euhedra in chlorite matrix - apparent layering, "graded bedding"
Granular Pyritic Mineralization	- μm- to mm-scale pyrite spheroids and spheroidal aggregates in matrix of sphalerite or gangue - internal colloform banding defined by porous pyrite, chalcopyrite, sphalerite, galena
Nodular Pyritic Mineralization	- mm- to cm-scale spherical bodies of pyrite in a sphalerite matrix - radiating internal structure
Massive Pyrite-Chalcopyrite	- massive pyrite with unoriented replacement veins of chalcopyrite or pseudomorphic replacement of colloform/spheroidal pyrite by chalcopyrite
Massive Fine Pyrite	- microcrystalline to cryptocrystalline pyrite - colloform textures defined by porous pyrite, minor chalcopyrite, galena, sphalerite
Massive Sphalerite	- massive fine-grained sphalerite
Banded Pyrite-Sphalerite	- bands of massive sphalerite up to 10 cm wide, alternating with bands of granular, massive, or nodular pyrite
Banded Pyrrhotite-Sphalerite	- bands of massive pyrrhotite interlayered with massive sphalerite
Banded Pyrrhotite-Pyrite	- bands of massive fine-grained pyrrhotite interlayered with granular pyrite
Stringer Mineralization	- veins, disseminations, and patches of chalcopyrite and/or pyrrhotite in altered wallrock
SECONDARY FACIES	Formed during metamorphism and deformation
Massive Coarse Pyrite	- massive coarse-grained pyrite with granuloblastic texture (triple junctions formed by recrystallization), some sutured grain boundaries
Foliated Mineralization	- transgressive wispy bands of fine, abraded pyrite and discontinuous bands of angular pyrite
Transgressive Veins and Breccia Zones	- subparallel and orthogonal sets of veins and veinlets, anastomosing networks of veinlets, vein breccias - contain any of pyrite, chalcopyrite, sphalerite, galena, electrum, quartz, chlorite, carbonate

* From Larocque *et al.* (1993a)

than cited previously (Fig. 5, Table 3). Details of data reduction are given in Appendix 1 of Larocque *et al.* (1995). In all, 178 analyses of pyrite in 78 sections, 59 analyses of chalcopyrite in 39 sections, and 15 analyses of pyrrhotite in 9 sections were carried out for different facies of mineralization from all three orebodies at the Mobrun mine. Ion-microprobe analyses of pyrite and chalcopyrite in samples from the Mobrun deposit had been carried out previously (Cook & Chryssoulis 1990). However, previous investigators analyzed samples from tailings, possibly resulting in a biased sample-population.

Results of Ion-Microprobe Analyses

Pyrite

The frequency diagrams of gold content of pyrite from the Main lens show log-normal distributions, with maxima in the 1–2 ppmw range (Fig. 6), similar to

TABLE 3. EXPERIMENTAL PARAMETERS FOR ION–MICROPROBE ANALYSIS

GENERAL PARAMETERS	
Instrument	Cameca IMS-4f ion microprobe
Standardization	external (ion implantation)
ION IMPLANTATION	
Ion source	low-pressure krypton dc thermal ionization source constructed at Chalk River Laboratories, Canada
Nominal ion energies	300 - 2000 keV
Operating ion energies	1 MeV
Implanted species	^{197}Au
Implantation dose	2.5E13 ions/cm^2
Mineral species	pyrite, chalcopyrite, pyrrhotite
OPERATING CONDITIONS	
Beam source	Cs
Primary-ion polarity	positive
Secondary-ion polarity	negative
Primary beam current	50 - 150 nA
Impact energy (primary ions)	5.5 keV (10 keV PAP[1], 4.5 keV SAP[2])
Sample-charge compensation	none
Primary-beam diameter	50 - 60 μm
Crater size	approximately 200 μm x 200 μm
Analysis diameter	60 μm
Mass interference	$^{197}CsS_2$
Energy offset	none
Mass resolution	2400 - 3900
Minimum detection limits (Au)	30 - 100 ppb
Depth of analyzed profile	0.3 - 1.3 μm
Dynamic range (peak/background)	3 decades

[1] Primary Accelerating Potential
[2] Secondary Accelerating Potential

results obtained by Cook & Chryssoulis (1990). The frequency distribution of gold content in pyrite from the Satellite lens complex is bimodal, with the principal maximum in the 1–2 ppmw range and a second maximum in the 8–16 ppmw range (Fig. 6). The frequency distribution for pyrite in the 1100 lens is bimodal, with the principal maximum in the 1–2 ppmw range and the second maximum in the 0.06–0.12 ppmw range (Fig. 6). The positive skew for samples from the Satellite lens complex may be due to sampling bias because the samples were selected for SIMS analysis on the basis of their high gold content in bulk assays, whereas assays for some samples from the 1100 lens were not known prior to doing SIMS analysis.

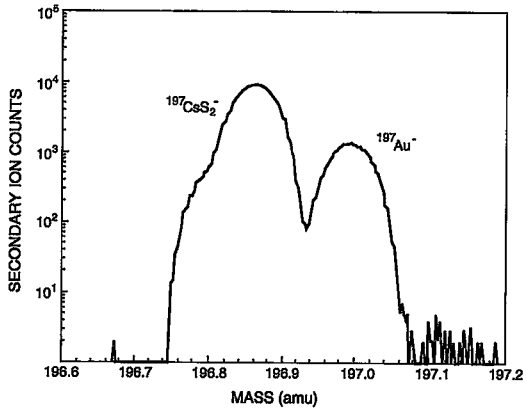

FIG. 4. High-mass-resolution spectrum showing Au peak and interfering mass ($^{197}CsS_2^-$)

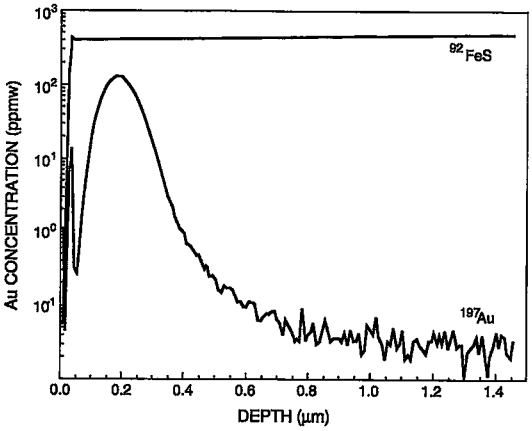

FIG. 5. SIMS depth-profile through external pyrite standard implanted with ^{197}Au. ^{92}FeS was monitored to ensure instrumental stability and sample homogeneity.

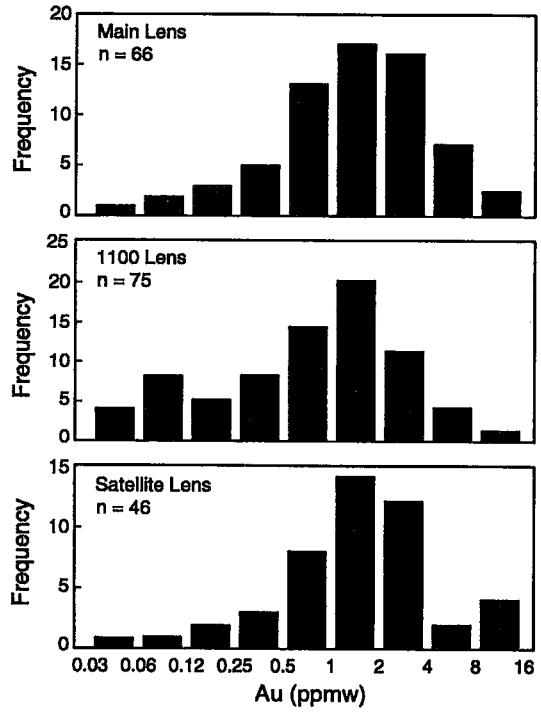

FIG. 6. Frequency distribution diagrams for gold content of pyrite (in ppmw), as determined by SIMS.

However, the 1100 lens has the lowest gold grades, and the Satellite lens complex has the highest gold grades (Table 1), consistent with the low and high second maxima and the low and high skewing of the principal maxima in the respective frequency-distributions (Fig. 6). Results of ion-microprobe analyses also are consistent with assays of hand specimens of ore (Larocque *et al.* 1993a).

The variable gold content of pyrite in different samples reflects the bulk zonation of gold throughout the orebodies. The reproducibility of analyses of pyrite in individual thin sections depends mainly on the textural homogeneity of pyrite. Table 4 summarizes the relationship between gold content and reproducibility of analyses in relation to facies of pyrite. In single sections containing homogeneous, inclusion-free, massive fine pyrite, the variation in gold content ranges from 0 to 20%. In sections containing granular pyrite, the variation in gold content ranges from 0 to 38%. Small spheroids of pyrite consistently have lower concentrations of gold than larger ones. In different thin sections from the same hand specimen, the variability in gold content of various facies of pyrite is as high as 50%.

Figures 7 shows the concentrations of "invisible" gold in pyrite in various facies of mineralization. The lowest concentrations of gold generally occur in massive recrystallized pyrite, whereas high concentrations of gold occur in granular and massive fine pyrite (Fig. 8). The spatial relationship among the various facies of mineralization in individual hand samples and thin sections is shown in Figures 2 and 3. The range of gold content in samples containing both primary and secondary facies of pyrite is much larger than those containing only primary facies. Massive recrystallized pyrite and pyrite in secondary veins *consistently* exhibit lower concentrations of gold than associated primary pyrite (Fig. 7). For example, recrystallized granular pyrite contains between 1 and 50% of associated primary concentrations of gold. Recrystallized massive pyrite contains between 1 and 67% of the gold concen-

TABLE 4. RANGE OF GOLD CONTENTS OF PYRITE (BY SIMS)

	Pyrite-Bearing Facies	Number of Analyses	Average Gold-Content (ppmw)	Mean Deviation (ppmw)	% Deviation
Main Lens					
1	granular	2	0.7	0.0	0
2	massive, slightly recrystallized py	2	4.5	0.5	11
3	massive fine py	2	3.5	0.5	14
4	massive fine py with inclusions	2	1.3	0.3	20
5	granular recrystallized py	2	1.1	0.0	0
6	massive recrystallized py	2	1.5	0.0	0
7	massive fine py with inclusions	2	2.1	1.0	46
8	massive fine py with inclusions	2	1.3	0.8	60
9	nodular py	2	2.0	0.0	0
10	granular py	2	1.5	0.5	33
11*	massive fine py	2	0.3	0.1	20
12	massive fine py	3	0.6	0.1	20
Satellite Lens Complex					
1	granular py with inclusions	3	1.5	0.0	0
2	granular py with inclusions	3	2.5	0.7	28
3#	granular py	2	1.6	0.6	38
4*	granular py with colloform cpy	2	10.5	0.5	5
5	granular py	2	0.9	0.2	18
6#	massive recrystallized py	2	0.5	0.1	20
7	massive fine colloform py	2	2.0	0.1	5
8*	massive fine py with inclusions	2	2.0	0.5	25
9	granular py	2	1.0	0.0	0
10	massive fine to granular py	2	1.0	0.0	0
11#	coarse granular py	2	1.5	0.0	0
12	fine granular py	2	0.5	0.0	0
13	massive fine py with inclusions	2	0.9	0.3	33
1100 Lens					
1#	granular py with fine inclusions	2	1.2	0.2	13
2*	granular py with coarse inclusions	2	3.0	0.5	17
3*	massive fine py	2	2.1	0.0	0
4*	massive recrystallized py with cpy	2	1.5	0.0	0
5	massive fine py	2	2.1	0.0	0
6#	massive fine py with inclusions	3	2.2	0.4	20
7	massive recrystallized py	3	0.4	0.2	50
8	massive fine py with inclusions	2	0.8	0.3	33
9	massive fine py with inclusions	2	1.5	0.0	0
10	massive fine py with inclusions	2	1.2	0.2	13
11	granular recrystallized py	2	0.5	0.1	20
12	massive, slightly recrystallized py	2	1.8	0.3	14
13	foliated py	2	0.2	0.1	33
14	massive fine py with inclusions	2	0.4	0.2	43
15	granular recrystallized py	2	0.4	0.0	0
16	massive coarse recrystallized py	2	0.0	0.0	25
17	massive fine py	2	0.4	0.0	0

same thin section as entry listed below
* same hand specimen as thin section listed below

trations in primary massive fine pyrite. The gold content of coarse euhedral pyrite in secondary veins ranges from 3 to 14% of that in associated massive fine pyrite. The large ranges of gold concentrations in secondary pyrite likely are a function of the degree of recrystallization, the lowest gold content being present in pyrite that has undergone the most extreme recrystallization (*e.g.*, coarse massive pyrite, and euhedral pyrite in veins).

With respect to the siting of gold in pyrite, it appears that two types of gold are present. Figure 9 shows two depth-profiles through pyrite, one of which is flat; the

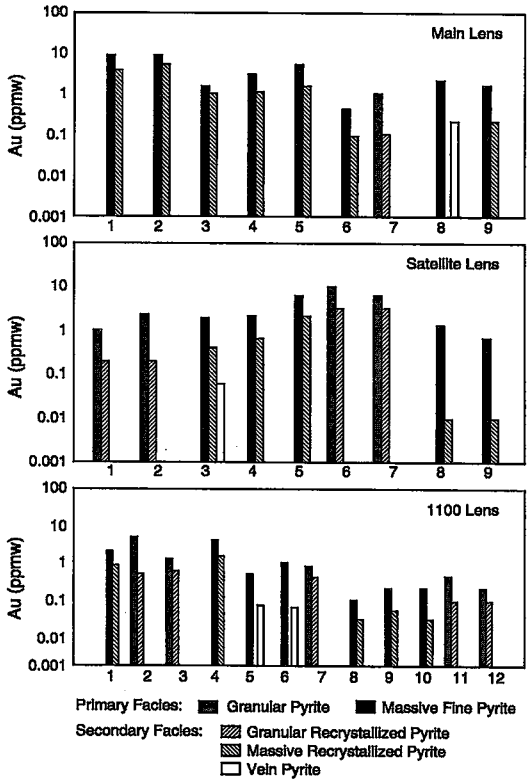

FIG. 7. Gold content of various pyrite-bearing facies coexisting within individual thin sections. Recrystallized massive pyrite and pyrite in secondary veins consistently exhibit lower concentrations of gold than associated primary pyrite.

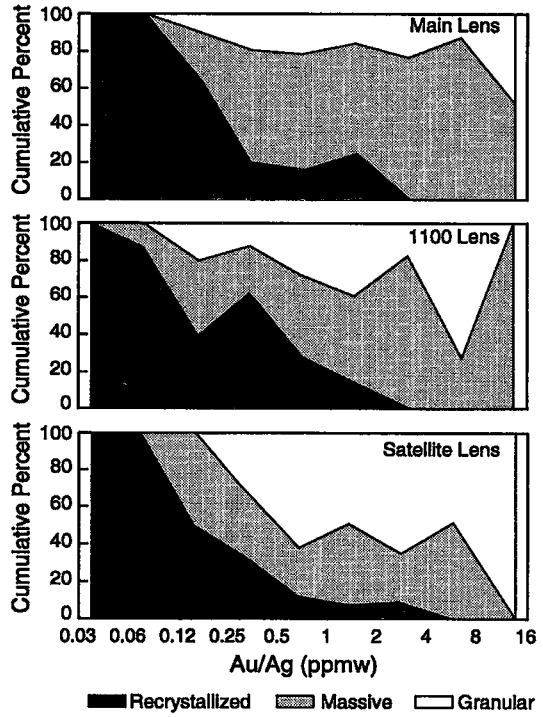

FIG. 8. Cumulative frequency diagram showing proportions of various pyrite-bearing facies within each concentration interval in Figure 6. Massive Fine and Granular Facies are primary facies; recrystallized facies is secondary.

other shows a distinct peak. The peak is caused by the presence of an inclusion of electrum about 0.2 μm in diameter. The flat profile represents the content of "invisible" gold (<0.1 μm; Haycock 1937), which consists of very fine colloid-size gold or structurally bound gold. Other types of analysis are needed to distinguish between these two possibilities (*cf.* Marion *et al.* 1992). The gold contents in Figures 6, 7 and 8 and Table 4 represent levels of "invisible" gold.

Chalcopyrite

Fewer analyses were done of chalcopyrite than of pyrite because of the relative proportion of each mineral in the deposit. It seems, however, that the frequency distributions of gold in chalcopyrite are different from those of gold in pyrite. Frequency distributions for pyrite in all orebodies show a maximum in the 1–2 ppmw range (Fig. 6). In contrast, the principal maxima in the frequency distributions of gold in chalcopyrite (albeit based on fewer samples) are variable (Fig. 10). The frequency distributions of gold in chalcopyrite in the Main and Satellite lenses show maxima in the 0.5–1 ppmw range, whereas the maximum for the 1100 lens is in the 0.06–0.12 ppmw range (Fig. 10).

Primary chalcopyrite occurs as thin colloform layers or fine grains intergrown with pyrite, and thus was too fine-grained to be analyzed with the 50 μm-diameter beam used for this study. Therefore, most of the chalcopyrite analyzed consists of coarse grains in secondary veins. However, analysis of pyrite with colloform bands or fine inclusions of chalcopyrite yielded higher concentrations of gold than associated "clean" pyrite, indicating that gold is present in primary chalcopyrite in higher amounts than in the associated pyrite. In addition, ion images of chalcopyrite veinlets emanating from primary colloform chalcopyrite in spheroidal aggregates of pyrite indicate the presence of gold in primary chalcopyrite (Fig. 11).

Pyrrhotite

Relatively few analyses of pyrrhotite were done, all of which were on samples from the 1100 lens; pyrrhotite is not present in the other orebodies. The low

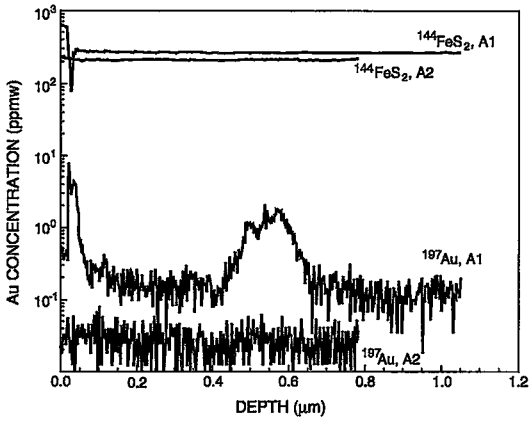

FIG. 9. SIMS depth-profiles through samples of pyrite from Mobrun. The peak in A1 is caused by an inclusion of electrum about 0.2 μm in diameter.

number of samples analyzed may account for the skewed distribution in gold content of pyrrhotite, which has a maximum in the 0.03–0.06 ppmw range (Fig. 12). This maximum is lower than the maxima in gold content of pyrite in any of the orebodies, and slightly lower than the maximum for gold-content of chalcopyrite in the 1100 lens.

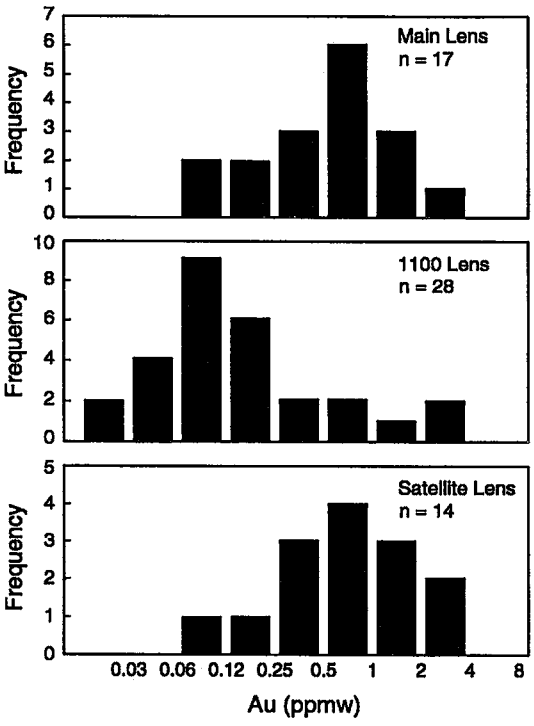

FIG. 10. Frequency-distribution diagrams for gold content of chalcopyrite as determined by SIMS.

DISCUSSION

The presence of significant amounts of gold in primary pyrite and chalcopyrite establishes unequivocally that *syngenetic gold is present in the Mobrun orebodies*. The fact that recrystallized pyrite contains less gold than the associated primary pyrite indicates that recrystallization resulted in the release of gold. It is possible that this release resulted from synvolcanic hydrothermal recrystallization (Huston *et al.* 1993). However, the presence of pressure-solution textures in pyrite and the occurrence of coarse euhedral pyrite on the margins of tectonic veins and oriented overgrowths on granular pyrite indicate that at least some recrystallization accompanied metamorphism and deformation (Larocque 1993, Larocque *et al.* 1993a). Thus, *metamorphic recrystallization resulted in the release of refractory gold from pyrite* and its subsequent deposition as electrum in tectonic veins.

Although electrum occurs in all three orebodies at Mobrun, it is most abundant and coarse grained in the 1100 orebody. This is partly due to the higher degree of recrystallization in the 1100 orebody relative to the other lenses, resulting in the liberation of a greater amount of gold. The results of the ion-microprobe analyses indicate that remobilized gold also may be deposited as "invisible" gold in secondary chalcopyrite. Unlike the frequency-distribution diagrams of gold in pyrite, which all have a maxima in the 1–2 ppmw range, the histograms showing the gold content of chalcopyrite exhibit different maxima, with the maximum for the 1100 lens being *an order of magnitude lower* than the maxima for the Main and Satellite lenses. This observation suggests that remobilized gold may have been partitioned differently during deposition from the metamorphic fluids affecting the different orebodies: in the Main and Satellite lenses, remobilized gold was deposited mainly in gold-rich chalcopyrite associated with minor electrum, whereas in the 1100 orebody, remobilized gold was deposited mainly as electrum in association with gold-poor chalcopyrite. The differences in host mineral and in

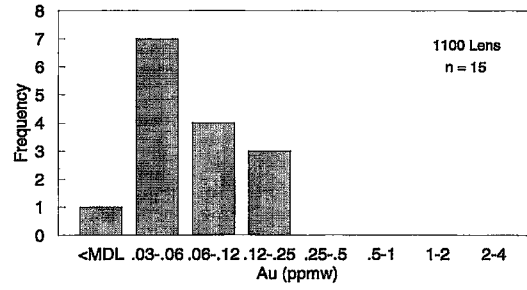

FIG. 12. Frequency-distribution diagram for gold content of pyrrhotite, as determined by SIMS.

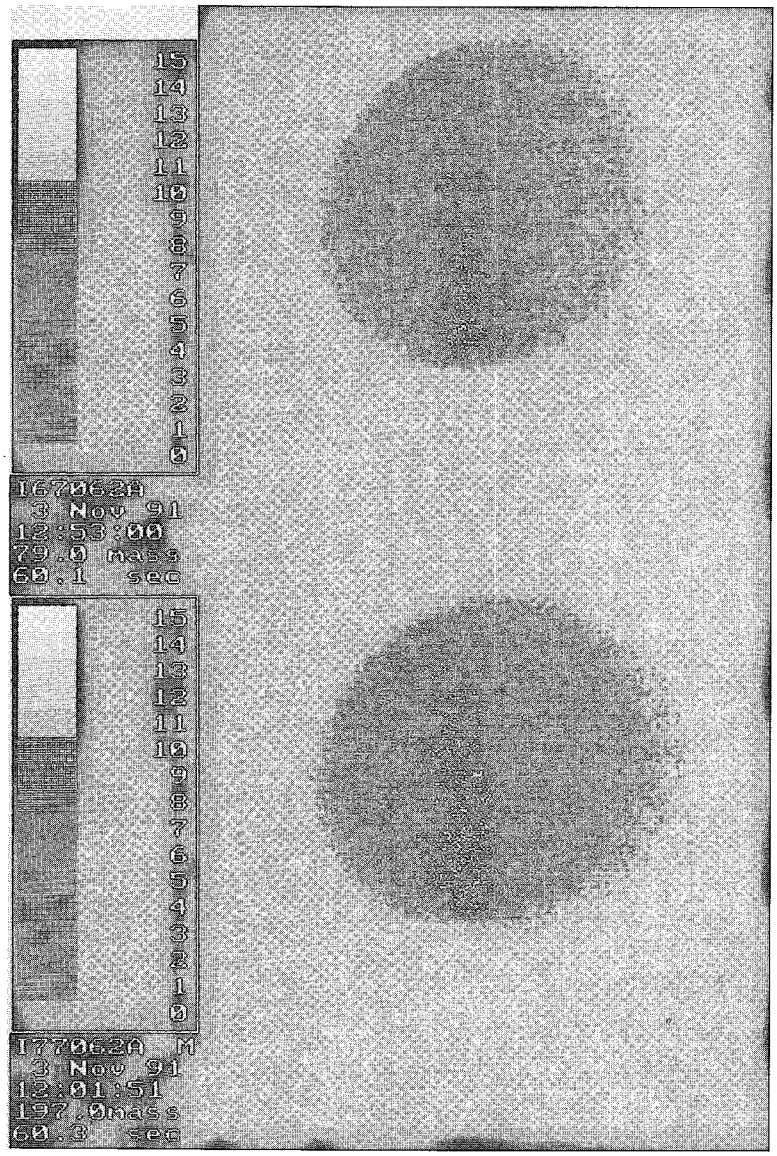

FIG. 11. Ion images for Cu (top) and Au (bottom) in chalcopyrite veinlet shown in Figure 3B. Scales at left correspond to secondary-ion counts.

degree of concentration of remobilized gold in the different orebodies may reflect differences in the sulfur activity of the remobilizing fluids, as the concentration of sulfide-held gold in equilibrium with free gold increases with increasing activity of sulfur in the fluid (Barton 1970). The stratigraphically lower part of the 1100 orebody is characterized by abundant pyrrhotite (stable under low activity of sulfur), whereas the iron sulfide in the Main and Satellite lenses is pyrite (stable under high activity of sulfur). The composition of the remobilizing fluid would have been influenced by its interaction with primary ore-mineral assemblages. Relatively gold-poor pyrrhotite would not have contributed much gold to the fluid, but would have influenced the activity of sulfur in the fluid, thereby increasing the stability of free gold relative to sulfide-held gold. Thus, differences between primary mineral assemblages of the orebodies may have exercised significant control on the partitioning of gold among secondary phases in each of the orebodies.

Our results are significant for a number of reasons. First, although the intensity of metamorphism at Mobrun is relatively low, metamorphic remobilization of gold has been demonstrated. The amount of gold released and the distances of transport were not large in the Main and Satellite lenses; in the 1100 lens, redistribution occurred on the scale of the orebody (Larocque *et al.* 1993a). However, *metamorphic recrystallization has been important in increasing the amount of cyanide-recoverable gold in the deposit.* Moreover, the fact that metamorphic remobilization has occurred at Mobrun suggests that some sulfide-rich gold deposits (*e.g.*, Bousquet, Dumagami) may have resulted from intense metamorphic reworking of primary gold-rich base-metal sulfide deposits like Mobrun (Tourigny *et al.* 1989, Larocque 1993, Larocque & Hodgson 1993).

Conclusions

(1) The presence of measurable quantities of gold in primary facies of mineralization establish that syngenetic gold is present in the Mobrun orebodies.
(2) "Invisible" gold in pyrite is present in submicroscopic inclusions of electrum and as fine colloid-size or structurally bound gold.
(3) Metamorphic recrystallization resulted in the release of "invisible" gold from pyrite, and was important in upgrading refractory gold in pyrite to a more easily recoverable form (electrum).
(4) Partitioning of remobilized gold between electrum and gold-bearing chalcopyrite may have been controlled by interaction of the metamorphic fluid with primary ore-assemblages.

Acknowledgements

We are grateful for the support of geological and mine personnel at Ressources Audrey Inc. and Mine Mobrun. Our research has benefitted from discussions with Michel Bouchard of Ressources Audrey Inc., Gérald Riverin of Minnova Inc., and Jim Franklin and Mark Hannington of the Geological Survey of Canada. At CANMET, Vic Chartrand provided capable technical assistance with ion-microprobe analysis. At Queen's University, Martin Burtt drafted some figures, and Tom Pearce kindly provided access to a photographic microscope. The manuscript was prepared while the first author was a guest scientist in Earth and Environmental Sciences Division, Group 1, at Los Alamos National Laboratory, New Mexico. Logistical support provided by EES–1 is greatly appreciated. The first author thanks Fraser Goff for his sponsorship and Jim Stimac for providing access to a photographic microscope. We thank Eric Montoya (EES–1) and Ruth Bigio (EES–4) for computer-aided drafting of figures. We are indebted to Tim Barrett, an anonymous reviewer, Associate Editor Frank Hawthorne and Editor Robert Martin for comments that improved the manuscript. Financial support was provided by Ressources Audrey Inc., Minnova Inc., and the Natural Sciences and Engineering Research Council of Canada, through a Collaborative Research and Development Grant awarded to CJH.

References

Arehart, G.B., Chryssoulis, S.L. & Kesler, S.E. (1993): Gold and arsenic in iron sulfides from sediment-hosted disseminated gold deposits: implications for depositional processes. *Econ. Geol.* **88**, 171-185.

_____, Kesler, S.E. & O'Neil, J.R. (1991): Elemental and sulphur isotopic zoning in iron sulfide grains from sediment-hosted micron gold deposits: implications for deposit genesis. *Geol. Soc. Am., Program Abstr.* **23**, A228.

Bakken, B.M., Brigham, R.H. & Fleming, R.H. (1991): The distribution of gold in unoxidized ore from Carlin-type deposits revealed by secondary ion mass spectrometry (SIMS). *Geol. Soc. Am., Program Abstr.* **23**, A228.

Barrett, T.J., Cattalani, S., Hoy, L., Riopel, J. & Lafleur, P.-J. (1992): Massive sulfide deposits of the Noranda area, Quebec. IV. The Mobrun mine. *Can. J. Earth Sci.* **29**, 1349-1374.

Barton, P.B., Jr. (1970): Sulfide petrology. *Mineral. Soc. Am., Spec. Pap.* **3**, 187-198.

Bischoff, J.L., Rosenbauer, R.J., Aruscavage, P.J., Baedecher, P.A. & Crock, J.G. (1983): Sea-floor massive sulfide deposits from 21°N, East Pacific Rise; Juan de Fuca Ridge; and Galapagos Rift: bulk chemical composition and economic implications. *Econ. Geol.* **78**, 1711-1720.

Cabri, L.J. (1992): The distribution of trace precious metals in minerals and mineral products. *Mineral. Mag.* **56**, 289-308.

_____ & Chryssoulis, S.L. (1990): Advanced methods of trace-element microbeam analyses. *In* Advanced Microscopic Study of Ore Minerals (J.L. Jambor & D.J. Vaughan, eds.). *Mineral. Assoc. Can., Short-Course Handbook* **17**, 341-377.

_____, _____, Campbell, J.L. & Teesdale, W.J. (1991): Comparison of *in-situ* gold analyses in arsenian pyrite. *Appl. Geochem.* **6**, 225-230.

_____, _____, de Villiers, J.P.R., Laflamme, J.H.G. & Buseck, P.R. (1989): The nature of "invisible" gold in arsenopyrite. *Can. Mineral.* **27**, 353-362.

Caumartin, C. & Caillé, M.-F. (1990): Volcanic stratigraphy and structure of the Mobrun mine. *In* The Northwestern Quebec Polymetallic Belt: a Summary of 60 Years of Mining Exploration (M. Rive, P. Verpaelst, Y. Gagnon, J.-M. Lulin, G. Riverin & A. Simard, eds.). *Can. Inst. Min. Metall., Spec. Vol.* **43**, 119-132.

CHRYSSOULIS, S.L. (1990): Quantitative trace precious metal analysis of sulfide and sulpharsenide minerals by SIMS. *In* Secondary Ion Mass Spectrometry, SIMS VII (A. Benninghoven, C.A. Evans, K.D. McKeegan, H.A. Storms & H.W. Werner, eds.). John Wiley & Sons, Ltd., Chichester, U.K. (405-408).

_____ & CABRI, L.J. (1990): Significance of gold mineralogical balances in mineral processing. *Inst. Min. Metall., Trans.* **99**, C1-10.

_____, _____ & LENNARD, W. (1989): Calibration of the ion microprobe for quantitative trace precious metal analyses of ore minerals. *Econ. Geol.* **84**, 1684-1689.

_____, _____ & SALTER, R.S. (1987): Direct determination of invisible gold in refractory sulfide ores (R.S. Salter, D.M. Wyslouzil & G.W. McDonald, eds.). *Proc. Int. Symp. on Gold Metallurgy*, **1**. Proc. Metall. Soc., Can. Inst. Min. Metall. (235-244).

_____, CHAUVIN, W.J. & SURGES, L.J. (1986): Trace element analysis by secondary ion mass spectrometry with particular reference to silver in the Brunswick sphalerite. *Can. Metall. Quart.* **25**, 233-239.

_____, SURGES, L.J. & SALTER, R.S. (1985): Silver mineralogy at Brunswick Mining and Smelting Corporation, Ltd. *In* Complex Sulfides (A.D. Zunkel, R.S. Boorman, A.E. Morris & R.J. Wesley, eds.). The Metall. Soc., Am. Inst. Mining Engineers (815-830).

COOK, N.J. & CHRYSSOULIS, S.L. (1990): Concentrations of "invisible gold" in the common sulfides. *Can. Mineral.* **28**, 1-16.

DE ROSEN-SPENCE, A.F. (1976): *Stratigraphy, Development and Petrogenesis of the Central Noranda Volcanic Pile, Noranda, Québec.* Ph.D. thesis, Univ. Toronto, Toronto, Ontario.

DIMROTH, E., IMREH, L., GOULET, N. & ROCHELEAU, M. (1983a): Evolution of the south-central segment of the Archean Abitibi Belt, Québec. II. Tectonic evolution and geomechanical model. *Can. J. Earth Sci.* **20**, 1355-1373.

_____, _____, _____ & _____ (1983b): Evolution of the south-central segment of the Archean Abitibi Belt, Québec. III. Plutonic and metamorphic evolution and geotectonic model. *Can. J. Earth Sci.* **20**, 1374-1388.

GÉLINAS, L., TRUDEL, P. & HUBERT, C. (1984): Chimicostratigraphie et tectonique du Groupe de Blake River. *Ministère de l'Energie et des Ressources du Québec*, **MM 83-01**.

GIBSON, H.L. & WATKINSON, D.H. (1990): Volcanogenic massive sulfide deposits of the Noranda cauldron and shield volcano. *In* The Northwestern Quebec Polymetallic Belt: a Summary of 60 Years of Mining Exploration (M. Rive, P. Verpaelst, Y. Gagnon, J.-M. Lulin, G. Riverin & A. Simard, eds.). *Can. Inst. Min. Metall., Spec. Vol.* **43**, 119-132.

HANNINGTON, M.D., HERZIG, P.M. & SCOTT, S.D. (1991): Auriferous hydrothermal precipitates on the modern seafloor. *In* Gold Metallogeny and Exploration (R.P. Foster, ed.). Blackie & Son, Glasgow, U.K. (249-282).

_____, PETER, J.M. & SCOTT, S.D. (1986): Gold in seafloor polymetallic sulfide deposits. *Econ. Geol.* **81**, 1867-1883.

_____ & SCOTT, S.D. (1988): Mineralogy and geochemistry of a hydrothermal silica – sulfide – sulfate spire in the caldera of Axial Seamount, Juan de Fuca Ridge. *Can. Mineral.* **26**, 603-625.

_____ & _____ (1989): Gold mineralization in volcanogenic massive sulfides: implications of data from active hydrothermal vents on the modern seafloor. *Econ. Geol., Monogr.* **6**, 491-507.

HAYCOCK, M.H. (1937): The role of the microscope in the study of gold ores. *Can. Inst. Min. Metall., Trans.* **40**, 405-414.

HEALY, R.E. & PETRUK, W. (1990): Petrology of Au–Ag–Hg alloy and "invisible" gold in the Trout Lake massive sulfide deposit, Flin Flon, Manitoba. *Can. Mineral.* **28**, 189–206.

HICKMOTT, D.D. & BALDRIDGE, W.S. (1991): PIXE and SIMS investigations of elemental and isotopic heterogeneities in coal sulfides and macerals. *Geol. Soc. Am., Program Abstr.* **23**, A465.

HUBERT, C., TRUDEL, P. & GÉLINAS, L. (1984): Archean wrench-fault tectonics and structural evolution of the Blake River Group, Abitibi Belt, Quebec. *Can. J. Earth Sci.* **21**, 1024-1032.

HUSTON, D.L. & LARGE, R.R. (1989): A chemical model for the concentration of gold in volcanogenic massive sulfide deposits. *Ore Geol. Rev.* **4**, 171-200.

_____, SIE, S.H., SUTER, G.F. & RYAN, C.G. (1993): The composition of pyrite in volcanogenic massive sulfide deposits as determined with the proton microprobe. *Nucl. Instrum. Methods Phys. Res., Ser.* **B75**, 531-534.

JOLLY, W.T. (1980): Development and degradation of Archean lavas, Abitibi area, Canada, in light of major element geochemistry. *J. Petrol.* **21**, 323-363.

KERR, D.J. & MASON, R. (1990): A re-appraisal of the geology and ore deposits of the Horne Mine complex at Rouyn–Noranda, Quebec. *In* The Northwestern Quebec Polymetallic Belt: a Summary of 60 Years of Mining Exploration (M. Rive, P. Verpaelst, Y. Gagnon, J.-M. Lulin, G. Riverin & A. Simard, eds.). *Can. Inst. Min. Metall., Spec. Vol.* **43**, 153-165.

LAROCQUE, A.C.L. (1993): *The Geologic Controls of Gold Distribution in the Mobrun Volcanic-Associated Massive Sulfide Deposit, Rouyn–Noranda, Quebec.* Ph.D. thesis, Queen's University, Kingston, Ontario.

———, CABRI, L.J., JACKMAN, J.A. & HODGSON, C.J. (1993c): SIMS analysis of Ag in pyrite: experimental parameters and preliminary results. *Geol. Assoc. Can. – Mineral. Assoc. Can., Program Abstr.* **18**, A56.

——— & HODGSON, C.J. (1991): Remobilization of ore constituents at the Mobrun Cu–Zn–Au mine in northwestern Quebec: preliminary observations from the Main and Satellite lenses. *Geol. Assoc. Can. – Mineral. Assoc. Can. – Soc. Econ. Geol., Program Abstr.* **16**, A71.

——— & ——— (1993): Carbonate-rich footwall alteration at the Mobrun mine, a possible Mattabi-type VMS deposit in the Noranda camp. *Explor. Mining Geol.* **2**, 165-169.

———, ———, CABRI, L.J. & JACKMAN, J.A. (1992): Application of SIMS analysis of pyrite to the study of metamorphic remobilization of Au in the Mobrun VMS deposit, Rouyn–Noranda, Quebec. *Geol. Assoc. Can. – Mineral. Assoc. Can., Program Abstr.* **17**, A63.

———, ———, ——— & ——— (1993b): Ion-microprobe study of sulphide minerals from the Mobrun VMS deposit in northwestern Quebec: evidence for metamorphic remobilization of Au. *Geol. Assoc. Can. – Mineral. Assoc. Can., Program Abstr.* **18**, A56.

———, ——— & LAFLEUR, P.-J. (1993a): Gold distribution in the Mobrun volcanic-associated massive sulphide deposit, Noranda, Quebec: a preliminary evaluation of the role of metamorphic remobilization. *Econ. Geol.* **88**, 1443-1459.

———, JACKMAN, J.A., CABRI, L.J. & HODGSON, C.J. (1995): Calibration of the ion microprobe for the determination of silver in pyrite and chalcopyrite from the Mobrun VMS deposit, Rouyn–Noranda, Quebec. *Can. Mineral.* **33**, 361-372.

LAYNE, G., HART, S.R. & SHIMIZU, N. (1991): Microscale lead and sulphur isotope zonation in hydrothermal sulfides by ion microprobe: new findings from the Mississippi Valley-type Pb–Zn deposits of the Viburnum Trend, S.E. Missouri. *Geol. Soc. Am., Program Abstr.* **23**, A101-102.

MARION, P., HOLLIGER, P., BOIRON, M.C., CATHELINEAU, M. & WAGNER, F.E. (1991): New improvements in the characterization of refractory gold in pyrites: an electron microprobe, Mössbauer spectrometry and ion microprobe study. *Proc. Brazil Gold '91* (E.A. Ladeira, ed.), 389-395.

———, MONROY, M., HOLLIGER, P., BOIRON, M.C., CATHELINEAU, M., WAGNER, F.E. & FRIEDL, J. (1992): Gold-bearing pyrites: a combined ion microprobe and Mossbauer spectrometry approach. *In* Source, Transport, and Deposition of Metals (M. Pagel & J.L. Leroy, eds.). Balkema, Rotterdam, The Netherlands.

MARQUIS, P., HUBERT, C., BROWN, A.C. & RIGG, D.M. (1990): An evaluation of genetic models for gold deposits of the Bousquet District, Quebec, based on their mineralogic, geochemical, and structural characteristics. *In* The Northwestern Quebec Polymetallic Belt: a Summary of 60 Years of Mining Exploration (M. Rive, P. Verpaelst, Y. Gagnon, J.-M. Lulin, G. Riverin & A. Simard, eds.). *Can. Inst. Min. Metall., Spec. Vol.* **43**, 383-399.

MCINTYRE, N.S., CABRI, L.J., CHAUVIN, W.J. & LAFLAMME, J.H.G. (1984): Secondary ion mass spectrometric study of dissolved silver and indium in sulfide minerals. *Scanning Elect. Micros.* **3**, 1139-1146.

NEUMAYR, P., CABRI, L.J., GROVES, D.I., MIKUCKI, E.J. & JACKMAN, J.A. (1993): The mineralogical distribution of gold and relative timing of gold mineralization in two Archean settings of high metamorphic grade in Australia. *Can. Mineral.* **31**, 711-725.

PENG, SHA (1992): SIMS analyses of gold in iron sulfides from the Gold Quarry Deposit, Nevada. *Geol. Soc. Am., Program Abstr.* **24**, A315-316.

RIOPEL, J., HUBERT, C., CATTALANI, S., BARRETT, T.J. & MACLEAN, W.H. (1990): *Métallogénie des Gisements de Métaux Usuels dans la Ceinture de Roches Vertes de l'Abitibi, Nord-Ouest Québécois. IV. La Mine Mobrun, Lentille Principale, Noranda, Québec.* IREM Projet No. 82-43G, 1988-89, Ministère de l'Energie et des Ressources, Québec.

SCOTT, S.D. & BINNS, R.A. (1992): An actively forming, felsic volcanic-hosted polymetallic sulfide deposit in the southeast Manus back-arc basin of Papua New Guinea. *EOS, Trans. Am. Geophys. Union* **73**, 626 (abstr.).

SPENCE, C.D. & DE ROSEN-SPENCE, A.F. (1975): The place of sulfide mineralization in the volcanic sequence at Noranda, Quebec. *Econ. Geol.* **70**, 90-101.

TOURIGNY, G., BROWN, A.C., HUBERT, C. & CRÉPEAU, R. (1989): Synvolcanic and syntectonic gold mineralization at the Bousquet mine, Abitibi greenstone belt, Quebec. *Econ. Geol.* **84**, 1875-1890.

———, DOUCET, D. & BOURGET, A. (1993): Geology of the Bousquet 2 mine: an example of a deformed, gold-bearing polymetallic sulfide deposit. *Econ. Geol.* **88**, 1578-1597.

Received June 10, 1993, revised manuscript accepted January 4, 1994.